Journal of Advanced Research (2016) 7, 297–304

Cairo University

Journal of Advanced Research

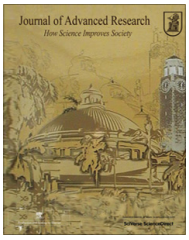

ORIGINAL ARTICLE

Porous bodies of hydroxyapatite produced by a combination of the gel-casting and polymer sponge methods

Jazmín I. González Ocampo *, Diana M. Escobar Sierra, Claudia P. Ossa Orozco

Biomaterials Research Group, Bioengineering Program, University of Antioquia, Street 70 # 52 – 21, Medellin 1226, Colombia

ARTICLE INFO

Article history:
Received 11 March 2015
Received in revised form 19 June 2015
Accepted 26 June 2015
Available online 3 July 2015

Keywords:
Gel-casting
Hydroxyapatite
Polymer sponge
Porous body

ABSTRACT

A combination of gel-casting and polymeric foam infiltration methods is used in this study to prepare porous bodies of hydroxyapatite (HA), to provide a better control over the microstructures of samples. These scaffolds were prepared by impregnating a body of porous polyurethane foam with slurry containing HA powder, and using a percentage of solids between 40% and 50% w/v, and three different types of monomers to provide a better performance. X-Ray Diffraction (XRD), and Fourier Transformed Infrared (FTIR) and Scanning Electron Microscopy (SEM) were employed to evaluate both the powder hydroxyapatite and the scaffolds obtained. In addition, porosity and interconnectivity measurements were taken in accordance with the international norm. Bioactivity was checked using immersion tests in Simulated Body Fluids (SBF). After the sintering process of the porous bodies, the XRD results showed peaks characteristic of a pure and crystalline HA (JCPDS 9-432) as a single phase. SEM images indicate open and interconnected pores inside the material, with pore sizes between 50 and 600 μm. Also, SEM images demonstrate the relatively good bioactivity of the HA scaffolds after immersion in SBF. All results for the porous HA bodies suggest that these materials have great potential for use in tissue engineering.

Introduction

Hydroxyapatite (HA), with a chemical composition of $Ca_{10}(PO_4)_6(OH)_2$, is a biocompatible and bioactive material with a similar crystal structure to the biological apatite that can be found in hard tissues such as teeth and bones [1]. It has been widely used in orthopedics and dentistry because of its close biocompatibility with the human body and its good integration with bones. Additionally, it offers diverse conformation possibilities, given that it is possible to manufacture

* Corresponding author. Tel.: +57 011 574 2198589.
E-mail address: jazmin.gonzalez@udea.edu.co (J.I. González Ocampo).

Peer review under responsibility of Cairo University.

http://dx.doi.org/10.1016/j.jare.2015.06.006

powder, coatings, dense bodies, and porous bodies [2–4]. As a result, it has been suggested that HA is the best substitute for bone.

HA is a ceramic material that exhibits low mechanical properties, in particular low tensile strength and fracture toughness. Its application is limited to human body parts subject to either reduced mechanical strain or compressive stress only [5]. Consequently, several material properties need to be modified, i.e. mechanical strength, solubility and sintering processes. This is achieved by controlling composition, morphology, and particle size [6,7].

In spite of the limitations listed above, the use of porous hydroxyapatite bodies to repair bone defects is now a common practice in tissue engineering. The porous bodies provide the basis for new tissue growth and features such as biocompatibility, biodegradability and bioactivity. Also, the presence of interconnected pores makes nutrient diffusion and vascular growth possible, as well as providing mechanical strength, migration, cell proliferation, and growth [8,9].

The formation of new bone depends greatly on pore characteristics such as porosity percentage, pore size, pore size distribution and pore shape. Such factors must be controlled to establish the relationship between key structural features (pore size, pore size distribution and interconnectivity) and the mechanical performance of these materials.

The aim of this work was to manufacture HA porous bodies employing the gel-casting technique combined with polymeric foam infiltration. This method has the advantage of allowing a high level of interconnectivity, and so provides a uniform distribution of porosity.

In relation to the formation mechanism of the ceramic porous body is given by the replication of the polymeric foam structure used as template once the ceramic slurry gets inside its porosity. Besides, the use of monomers in gel-casting technique generates a 3D network that provides a temporary support to the HA particles. Both polymeric elements -monomers and polymeric foam- are completely burned when the bodies are sintered, providing cavities or porosities to the new only-ceramic structure granting not only an open and interconnected porosity, but also a uniform particle distribution [6,10,11]. Three different monomers and 40% and 50% w/v of HA solids were used to achieve the optimum values for some of the properties required in tissue engineering, such as morphology, pore size, bioactivity, percentage of porosity and interconnectivity. This report is the first to evaluate the behavior of porous bodies when varying the type of monomer and percentage of solids used.

Material and methods

Characterization of hydroxyapatite powder

The hydroxyapatite powder used as a raw material was evaluated by Fourier Transform Infrared Spectroscopy – FTIR – (Perkin Elmer Spectrometer – model Spectrum One detector DTGS). A wave range number of 4000–400 cm^{-1} was used. X-Ray Diffraction analysis was performed with a diffractometer (Brand Rigaku) and a copper (Cu) target as follows: λ = 1.5818 Å; angle 2θ; angle range of 0–60°.

Table 1 Sample nomenclature.

Sample	Nomenclature
40% of solids and Methacrylamide	40HAM
40% of solids and Acrylamide	40HAA
40% of solids and N-methylolacrylamide	40HAN
50% of solids and Methacrylamide	50HAM
50% of solids and Acrylamide	50HAA
50% of solids and N-methylolacrylamide	50HAN

Manufacture of porous bodies

Commercial hydroxyapatite powder from Strem Chemicals was used for the manufacturing process. The average particle size was 12.9 μm. The porous bodies were made according to the gel-casting technique combined with polymeric foam infiltration. Methacrylamide, Acrylamide, and N-methylolacrylamide were employed as functional monomers and the HA percentages were 40% and 50% w/v. The nomenclature of the samples employed is shown in Table 1.

Initially, a Velp Scientifica Arex magnetic agitator was used to mix the following substances for 3 min until a homogeneous solution was achieved: distilled water, the functional monomer, bisacrylamide (crosslinker), polyvinyl alcohol (binder), and methacrylic acid (dispersant). Afterward, the solution was mixed with hydroxyapatite powder in a Kika Labortechnik RW mechanical mixer for 15 min to break the agglomerates present in the powder. Next, the existing bubbles were removed from the mixture in a vacuum chamber. The catalyst and the initiator were then added and the homogenization was continued for another 5 min. Once the mixture was ready, infiltration inside the suspension of polyurethane foams was performed. The foams were left inside the chamber for 30 min so the polymerization process could be completed. Thermal treatment was then carried out, beginning with drying at room temperature for 24 h in order to eliminate the excess water. Samples were then dried in a Blinder model 53 ED drying oven at 70 °C for 15 h, thus producing a mechanic strength that enabled the samples to be handled. Finally, the samples were sintered at 1200 °C for 3 h.

Polyurethane foam was selected in accordance with preliminary tests and commercial grade was chosen to make it affordable. The selected foam presented a pore size average of 500 μm, wall thickness of approximately 150 μm, and interconnectivity, as shown in Fig. 1.

Characterization of porous bodies

For the characterization of the porous bodies, several tests were carried out using Scanning Electron Microscopy (SEM) with a JEOL microscope (model JSM-6490LV), and X-Ray Diffraction (XRD) using a Rigaku diffractometer with a copper (Cu) source (λ = 1.5818 Å, at an angle of 2θ and in a range of 0–60°). Bioactivity essays were then undertaken using immersion tests in simulated body fluid (SBF), in accordance with the procedure used by Kokubo and Takadama [12]. To verify the formation of the apatite layer formed on the surface, Ca/P of this was evaluated by energy dispersive spectroscopy (EDS) in JEOL microscope (model JSM-6490LV). In

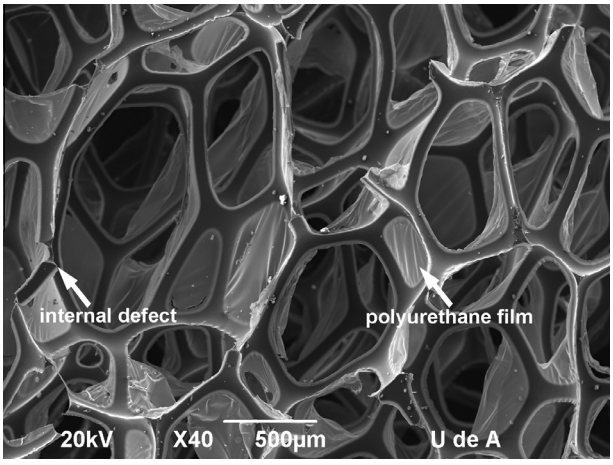

Fig. 1 Micrograph of polyurethane foam.

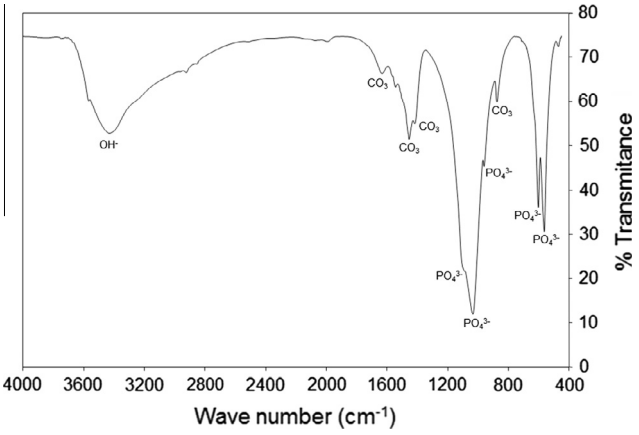

Fig. 2 Infrared spectrum via Fourier transform for the hydroxyapatite powder.

Addition, porosity and interconnectivity tests were performed following the methodology reported by Liu and Miao [13]. Initially, the net weight of the sample (W_{net}) was obtained, and then the sample was saturated with distilled water according to the ISO 10545-3 standard.

Eqs. (1)–(4) were used to obtain the total porosity (Φt), open porosity (Φ_a), mass porosity (Φ_m) and interconnectivity of the pores (p_i).

$$\Phi_a = \frac{W_{sat} - W_{net}}{\rho_a V} \tag{1}$$

$$\Phi_m = \frac{(W_{sat} - W_{net})100}{W_{net}} \tag{2}$$

$$\Phi t = 1 - \frac{\rho}{\rho^*} \tag{3}$$

$$p_i = \frac{\Phi_a}{\Phi_t} \tag{4}$$

Where V is the volume of the porous body, ρ is the real density of the material, ρ^* is the apparent density of the porous body, and ρ_a is the density of water.

Statistical analysis

Experimental data were presented as mean ± SD (standard deviation). Statistical analysis of the data was performed using the one-way ANOVA with Statgraphics Centurion 16 software. The differences were considered to be significant at a level of $p < 0.05$.

The experimental design input factors were the HA percentage (40% and 50% w/v) and the kind of monomer (Methacrylamide, Acrylamide and N-methylolacrylamide). The response was total porosity and interconnectivity. All experiments were performed maintaining the binder, surfactant, dispersant, crosslinker monomer, initiator, and catalyst as constants.

Results and discussion

Characterization of the HA powder

Fig. 2 shows the characteristic peaks of the HA powder analyzed in the infrared spectrum. The bands at 1650 and 3470 cm^{-1} correspond to H_2O absorption, the bands at 1034, 602 and 563 cm^{-1} are characteristic of phosphate bending vibration, while the band at 980 cm^{-1} is attributed to phosphate stretching vibration. The bands at 1455, 1414 and 874 cm^{-1} are indicative of carbonate ion substitution. The analyses of these bands confirmed that the spectra shown in Fig. 2 belong to HA. No functional groups were found which can affect the behavior of the manufactured porous bodies [14].

Fig. 3 shows the diffractogram acquired for the HA powder. The main high values of a typical HA are observed at $2\theta = 31.7°$, 32.2° and 33°. Secondary high points with less intensity are located at $2\theta = 26.4°$, 46.5° and 49°. The JCPDS 9-432 pattern confirms the presence of HA. Other peaks found at $2\theta = 29°$ and $2\theta = 53.2°$ correspond to a small quantity of α-tricalcium phosphate (α-TCP) (JCPDS 29- 359). However, this does not represent a significant source of contamination, since after the porous bodies are manufactured they pass through the sintering, where this phase is transformed into HA, as seen in Fig. 5. The powder is highly crystalline, which is one of the main factors responsible for the good performance of the implant *in vivo* [15].

Characterization of porous bodies

The micrographs of the porous bodies for the three different types of assessed monomers and different percentages of solids are shown in Fig. 4. The SEM micrographs show open and interconnected pores inside the material. They have a pore size between 100 and 600 µm and an irregular geometry, as well as internal pores of a lesser size with values between 50 and 100 µm. This suggests the existence of an internal microporosity in the ceramic materials with interconnectivity for values above 10% porosity as Teixeira et al. [16] reported. Moreover, the surface of the porous bodies is rough, favoring cellular adhesion and inducing new bone formation [11,13].

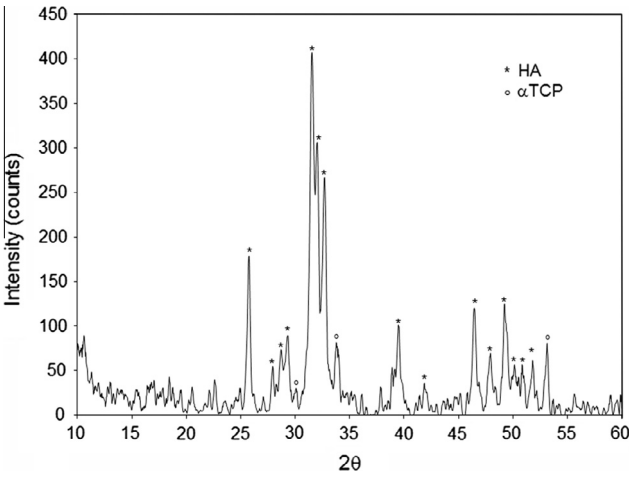

Fig. 3 Hydroxyapatite powder diffractogram.

The structure of the porous bodies is similar to the trabecular bone in terms of porosity and interconnectivity [17]. In accordance with work carried out by Ramay and Zhang [11], the scaffolds require these parameters to have a similar composition and pore morphology. This reproduces the bone characteristics necessary in tissue engineering to promote vascularization and good implant integration. Before the aforementioned morphological characteristics were observed in the porous bodies, there was a structure consisting of a network of interconnected pores with a rough texture.

The pore size plays a key role in the design of scaffolds, since bone regeneration is directly affected. 5 μm pores permit new vascularization, pores between 15 μm and 40 μm allow fibroblastic growth, pores between 40 μm and 100 μm favor osteoid growth, pores between 200 μm and 350 μm allow significant bone growth and pores bigger than 500 μm permit fast vascularization. In addition, if the pores are interconnected, there is a higher degree of bone tissue penetration [9]. The literature reports that the optimum pore size for osteoconduction is 150–600 μm. The pore size and interconnecting structure obtained in this research (Fig. 4) are between 50 μm and 600 μm, which seems to be an appropriate range for porous materials with bone conducting potential and suitable for osteoblasts to grow into the scaffold for rapid vascularization.

The XRD results after the sintering process of the porous bodies can be seen in Fig. 5. The diffractogram pattern of the hydroxyapatite is presented along with diffractograms related to samples prepared with: Methacrylamide, acrylamide, N-methylolacrylamide, and the percentages of solids corresponding to each one. The diffraction results for the assessed porous bodies show the presence of principal peaks of intensity at $2\theta = 31.6°$, 32.2° and 33°. There are other peaks with lower intensities of $2\theta = 26°$, 34°, 40°, 46.5° and 49° and secondary peaks at $2\theta = 28.8°$, 39.2°, 50.5°, 52° and 53.2°. All of these are in agreement with the characteristic peaks of a pure and crystalline HA (JCPDS 9-432), indicating that the sintering process did not change the composition of HA.

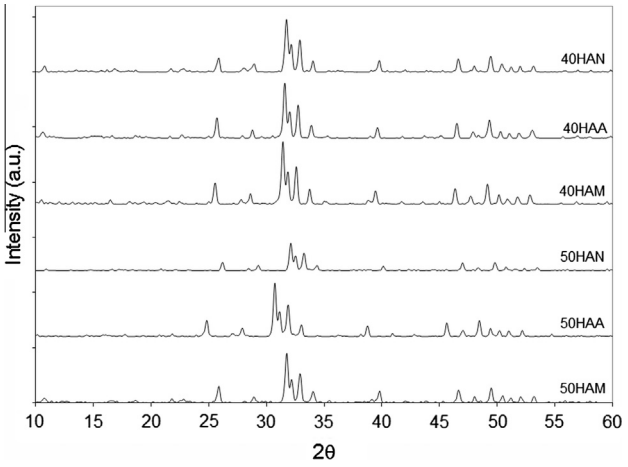

Fig. 5 X-Ray diffraction of the porous bodies for 40% and 50% of hydroxyapatite and the three monomers.

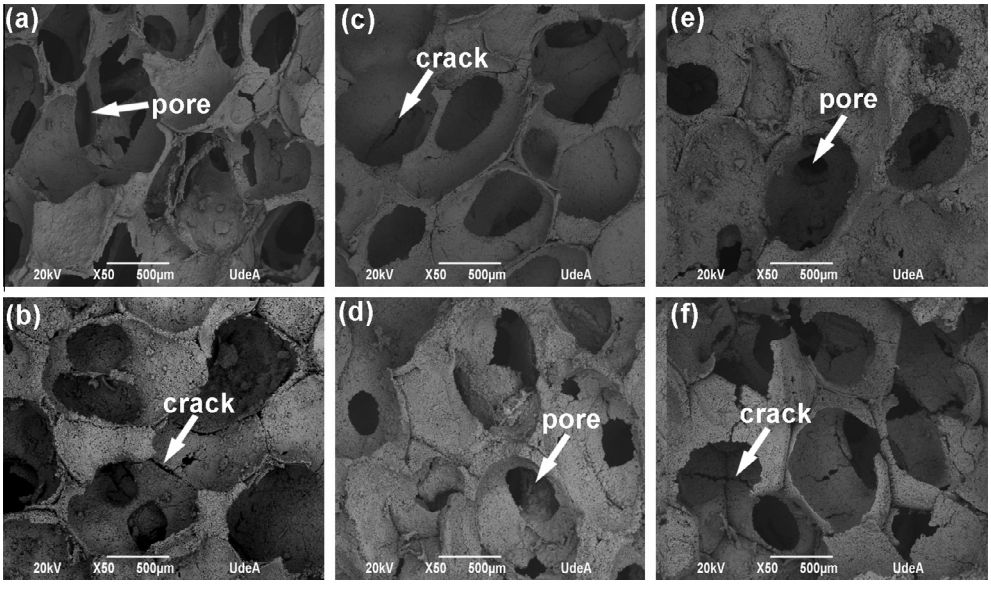

Fig. 4 Micrographs of the HA porous bodies, 50×: (a) 40HAM, (b) 50HAM, (c) 40HAA, (d) 50HAA, (e) 40HAN, (f) 50HAN.

Peaks for the 50HAA and 50HAN samples have a displacement relative to the standard conditions (JCPDS 9-432). However, the relative intensity of peaks and crystallinity remain. This error in the position of the diffraction peaks may be due to movement of the sample relative to the axis of the diffractometer. Nevertheless, after thermal treatment all samples can be considered to have HA as a single phase. The other chemical reagents used in this process were eliminated during firing, and the sintered material is potentially non-toxic to living tissues. This allows the material to be used for biomedical applications.

The surface of porous bodies of HA immersed in SBF can be observed in the micrographs, which show the formation of apatite from the first day of immersion (Figs. 6 and 7). The mechanism of apatite formation in materials soaked in SBF has been described by many researchers [12,18]. It is known that once the apatite nuclei are formed, they can grow by consuming the calcium and phosphate ions present in the SBF. The scaffold surface morphology was changed and the porosity was reduced as a result of apatite deposition. The growth of apatite crystals fills the small pores, in turn reducing the size of the large pores, as reported by Ghomi et al. [19]. By day 21, the new apatite is deposited as layers, generating a 3D network. As shown in Fig. 8, all samples have porosities above 80% and the whole surface is covered by apatite. This is in agreement with the results reported by Dash et al. [20] who observed a high rate of formation of biologically active bonelike apatite in high porosity samples. Such observations are related to the rapid dissolution of calcium and phosphorus ions and their migration through an interconnected network of pores [21] that also have a high surface area. Apatite formation was also benefited by the interconnectivity of the samples produced by a combination of the gel-casting and polymer sponge methods, reaching values above 50%.

EDS showed that the Ca/P molar ratio was 1.61, very close to non-stoichiometric hydroxyapatite present in hard tissues [20], with this result and the morphology observed in the micrographs (Figs. 6 and 7), confirming then that the layer deposited is apatite.

The fact that these bodies permit the formation of HA on the surface suggests that they have great potential for use in tissue engineering. If a material is able to produce apatite on

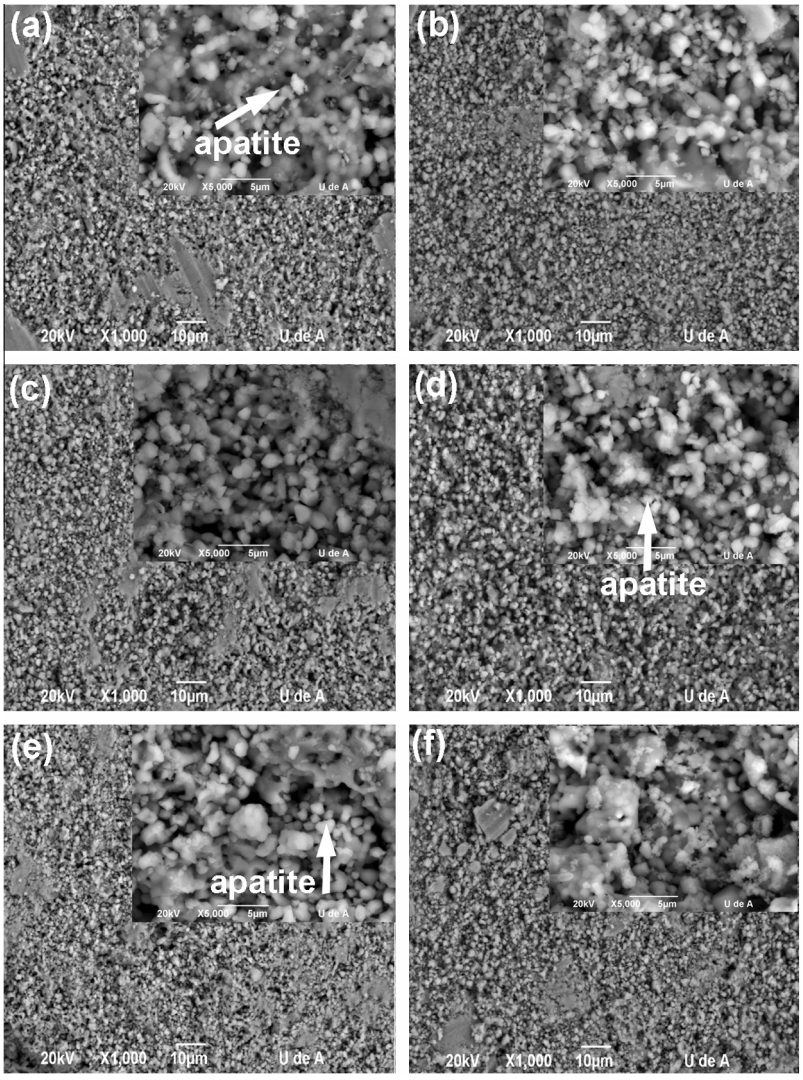

Fig. 6 SEM micrographs of the surfaces of the porous bodies immersed in SBF magnified 1000×. (a) Day 1 with 40HAM, (b) day 21 with 40HAM, (c) day 1 with 40HAA, (d) day 21 with 40HAA, (e) day 1 with 40HAN, (f) day 21 with 40HAN.

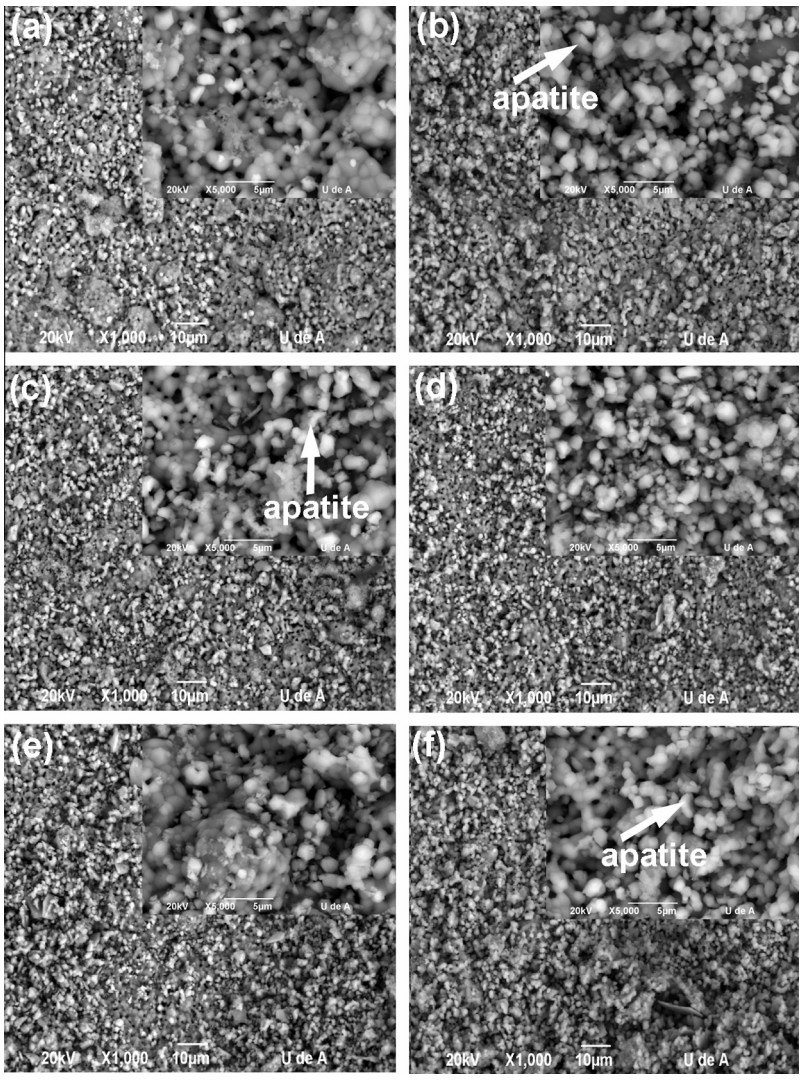

Fig. 7 SEM Micrographs of the surfaces of the porous bodies immersed in SBF magnified 1000×. (a) Day 1 with 50HAM, (b) day 21 with 50HAM, (c) day 1 with 50HAA, (d) day 21 with 50HAA, (e) day 1 with 50HAN, (f) day 21 with 50HAN.

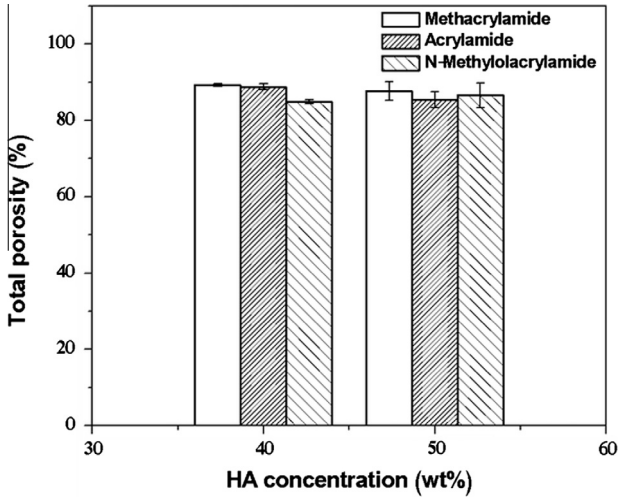

Fig. 8 Total porosity versus the amount of hydroxyapatite for the three types of monomers.

the surface through SBF, it will also be possible to produce apatite on an implant inside the human body, in turn aiding the chemical interaction between the implant and the host tissue [12]. Numerous studies have shown that apatite formation on the surface of materials is indicative of a bioactivity potential *in vivo* [22].

Some monomers could potentially irritate the human body. Therefore, in order for stable components to be obtained, it is necessary that the monomers undergo complete polymerization and curing [23]. In the case of foam processing, due to low evaporation point of polyurethane foam and monomers, they should volatilize during sintering in concordance with Ramay and Zhang [11], who report burn temperature for polyurethane foam as 500 °C and with Callcut and Knowles [24] who reported a temperature at 600 °C. XRD (Fig. 5) shows that HA is the only phase present. The monomers were volatilized, which suggests that there will be an appropriate response in future biocompatibility tests performed to confirm the use of this material as an implant.

The spherical precipitates present in all foams are characteristic of carbonated apatite $(Ca,Na)_{10}(PO_4,CO_3)_6(OH)_2$. Carbonated apatite is formed at 37 °C and pH 7.5 [25] after cationic exchange when the surface has contact with SBF ions. The same conditions were used in this assay. As observed in the XRD analysis (Fig. 5), all samples have the same initial phase before immersion. Accordingly, the dissolution rates are similar and the saturation levels of the SBF solution also are equivalent, meaning that the apatite layer has analogous characteristics. The generation of this apatite on the surface has a beneficial effect on cell adhesion during implantation.

The total porosities of the samples with the three types of monomers and two HA percentages are presented in Fig. 8.

ANOVA variance analysis was conducted to analyze porosity, from which two null-value hypotheses were established. The first was the equality of the porosity measurements for the porous bodies manufactured with the three types of monomers. The second was the two values of HA percentages used. A $p > 0.05$ was found for a HA percentage and the type of monomer. Consequently, it is inferred that none of these factors have a statistically significant effect on the porosity of the porous bodies.

In all cases, the porosity has the same order of magnitude. Moreover, the values are very close to each other, within a range of 84.9–89.2%. This is due to the polyurethane foam, which creates the porosity and is used as a template for the manufacturing process. A high porosity usually means there is a high surface area/volume ratio, and thus favors cell adhesion to the scaffold and promotes bone tissue regeneration [11].

All the porous bodies were made with the same type of foam. The minimal variations were due to small internal changes in the foam. Although the same foam was used in all cases, it may not have a strict porosity pattern and could have structural defects due to its commercial nature, as can be seen in Fig. 1 (arrows). Nonetheless, the use of different polymers in the amide group could generate a more stable 3D network, permitting a more homogenous placing of the HA particles. This, in turn, could improve the porosity, interconnectivity and mechanical properties of the material [11]. According to the literature reports, the porosity of trabecular bone, chiefly due to the wide vascular and bone marrow intertrabecular spaces, ranges from 30% to more than 90% [26]; furthermore, bone porosity is not fixed and can change in response to altered loading, disease, and aging. The results of this research are within that range, also they are consistent with the results presented by Imwinkelried [27], who studied about materials for bone repair compared to Ti foams with bone properties, and it was found that values above 80% porosity were optimal for use in bone applications with trabecular bone.

In Fig. 9, the interconnectivity of the samples with the three types of monomers and two percentages of hydroxyapatite can be observed. ANOVA and two null-value hypotheses were carried out. The first hypothesis was regarding the equality of the interconnectivity measurements for the porous bodies manufactured with the three types of monomers. The second featured the two values of HA percentages used. A $p > 0.05$ was found for the HA percentage and the type of monomer. Therefore, it can be inferred that none of these factors have a statistically significant effect on the porosity of the porous bodies.

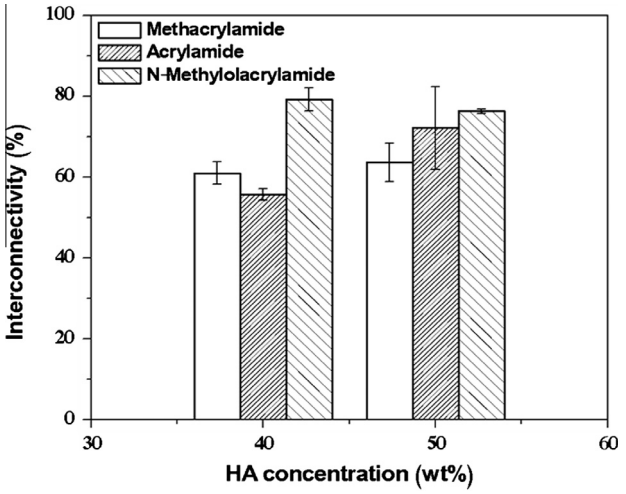

Fig. 9 Interconnectivity versus the amount of hydroxyapatite for the three types of monomers.

The interconnectivity of the samples can be observed, within a range of 55.8–79.2%, and it was statistically demonstrated that there is not a notable variation in interconnectivity with respect to the HA percentage and the type of monomer. This indicates that only the foam used as a template, which was injected with the chemical suspension, could influence this interconnectivity. Fig. 1 shows some pores obstructed in a polyurethane film which was later impregnated by the ceramic slurry. In some cases the walls may stay firm inside the structure or the space may be occupied by the polymer remains, leaving an internal defect after thermal treatment. The wall that separates the pores could break, given that it is so thin, producing a more interconnected structure. Furthermore, air bubbles trapped in the slurry can lead to closed pores with thin walls in the ceramic structure after drying. These walls can snap off, and generate a more interconnected structure [11]. The difference between the interconnectivity values of 40HAA and 40HAN may be due to the presence of the –OH group, making it more hydrophilic and causing the molecules to have less affinity with the crosslinking agent. Therefore, the structure could be more open and have higher interconnectivity values. Nevertheless, it was statistically demonstrated that all the mean interconnectivity values and porosities are the same. The interconnected porosity of the trabecular bone is between 50% and 70% [28]. Therefore, in terms of interconnectivity, the porous bodies provide the material with good properties for trabecular bone repair, because it can allow osteoconductivity, bone ingrowth and angiogenesis.

Conclusions

Using the gel-casting technique combined with the infiltration of polymeric foams, it was statistically demonstrated that the percentage of solids and the type of monomer did not have a significant effect on the porosity and interconnectivity of the samples. Since these properties are directly affected by the type of foam used as a template, it is very important to use foam with a known porosity and interconnectivity pattern.

The porous bodies internally possess macro-pores and micro-pores. The pore size is between 100 and 600 μm and the internal pore size is between 50 and 100 μm. This was corroborated by porosity and interconnectivity results that showed values from 84.9% to 89.2% and 55.8% to 79.2% respectively, which are very similar to the values of the trabecular bone.

The behavior exhibited by all of the porous bodies confirms their bioactivity. There were no monomers in the final foams which could generate sensitization and irritation reactions. This demonstrates the great potential that these bodies have for use in tissue engineering.

Conflict of Interest

The authors have declared no conflict of interest.

Compliance with Ethics Requirements

This article does not contain any studies with human or animal subjects.

Acknowledgments

The authors of this research thank the University of Antioquia -CODI- Research Committee for funding the development of the project: "Synthesis and Characterization of Porous Hydroxyapatite Bodies Obtained by Different Production Techniques". They also wish to thank the company Colorquímica S.A. for donating the monomers.

References

[1] Villora JM, Callejas P, Barba MF. Métodos de síntesis y comportamiento térmico del Hidroxiapatito. Boletín La Soc Española Cerámica Y Vidr 2002;41:443–50.
[2] Zyman Z, Glushko V. Nonstoichiometric hydroxyapatite granules for orthopaedic applications. Sci Mater Med 2004;15:551–8.
[3] Rodríguez R, Gómez J, Rodríguez R, Blardoni F. Biomaterial de restauración ósea. Rev Cuba Investig Biomédica 1999;18:203–7.
[4] Vallecillo M, Romero N, Pardo A. La hidroxiapatita en reconstrucción de defectos óseos de los maxilares: estudio y seguimiento de 15 casos clínicos. Rev COE 1999;4:137–43.
[5] Black J, Hastings G. Handbook of biomaterials properties. 1st ed. Londres: Chapman & Hall; 1998.
[6] Dhara S, Kamboj R, Pradhan M, Bhargava P. Shape forming of ceramics via gel-casting of aqueous particulate slurries. Bull Mater Sci 2002;25:565–8.
[7] Sepúlveda P. Processing of cellular ceramics synthesized by Gelcasting of foams. University of Nottingham; 1996.
[8] Dutta T, Simon J, Ricci J, Rekow E, Thompson V. Performance of hydroxyapatite bone repair scaffolds created via three-dimensional fabrication techniques. J Biomed Mater Res A 2003;67A:1228–37.
[9] Cunningham E, Dunne N, Walker G, Maggs C, Wilcox R, Buchanan F. Hydroxyapatite bone substitutes developed via replication of natural marine sponges. J Mater Sci Mater Med 2010;21:2255–61.
[10] Sepulveda P, Binner JG. Processing of cellular ceramics by foaming and in situ polymerisation of organic monomers. J Eur Ceram Soc 1999;19:2059–66.
[11] Ramay HR, Zhang M. Preparation of porous hydroxyapatite scaffolds by combination of the gel-casting and polymer sponge methods. Biomaterials 2003;24:3293–302.
[12] Kokubo T, Takadama H. How useful is SBF in predicting in vivo bone bioactivity? Biomaterials 2006;27:2907–15.
[13] Liu J, Miao X. Porous alumina ceramics prepared by slurry infiltration of expanded polystyrene beads. J Mater Sci 2005;40:6145–50.
[14] Londoño E, Echavarría A, De La Calle F. Características cristaloquímicas de la hidroxiapatita sintética tratada a diferentes temperaturas. Rev EIA 2006:109–18.
[15] Navarro ME. Desarrollo y Caracterización de Materiales Biodegradables para Regeneración Ósea. Universidad Politécnica de Cataluña; 2005.
[16] Teixeira S, Rodriguez M a, Pena P, De Aza a H, De Aza S, Ferraz MP, et al. Physical characterization of hydroxyapatite porous scaffolds for tissue engineering. Mater Sci Eng C 2009; 29: 1510–4.
[17] Montufar EB. Espumas inyectables de hidroxiapatita obtenidas por el método de espumado de la fase líquida de un cemento de fosfato tricálcico alfa. Universidad Politécnica de Cataluña; 2010.
[18] Kim H-M, Himeno T, Kokubo T, Nakamura T. Process and kinetics of bonelike apatite formation on sintered hydroxyapatite in a simulated body fluid. Biomaterials 2005;26:4366–73.
[19] Ghomi H, Fathi MH, Edris H. Effect of the composition of hydroxyapatite/bioactive glass nanocomposite foams on their bioactivity and mechanical properties. Mater Res Bull 2012;47:3523–32.
[20] Dash SR, Sarkar R, Bhattacharyya S. Gel casting of hydroxyapatite with naphthalene as pore former. Ceram Int 2014:1–16.
[21] Swain SK, Bhattacharyya S, Sarkar D. Preparation of porous scaffold from hydroxyapatite powders. Mater Sci Eng C 2011;31:1240–4.
[22] Ducheyne P, Qiu Q. Bioactive ceramics : the effect of surface reactivity on bone formation and bone cell function. Biomaterials 1999;20.
[23] Janney MA, Omatete OO, Walls CA, Nunn SD, Ogle RJ, Westmoreland G. Development of low-toxicity gelcasting systems. J Am Ceram Soc 1998;81:581–91.
[24] Callcut S, Knowles JC. Correlation between structure and compressive strength in a reticulated glass-reinforced hydroxyapatite foam 2002;3:485–9.
[25] LeGeros RZ. Calcium phosphates in oral biology and medicine. Monogr Oral Sci 1991;15.
[26] Bonucci E. Basic structure and composition of bone. In: Mechanical testing of bone and the bone-implant interface. In: An YH, Draughn RA, editors. Basic compos struct bone. Boca Raton: CRC Press; 2000. p. 3–22.
[27] Imwinkelried T. Mechanical properties of open-pore titanium foam. J Biomed Mater Res Part A 2007;81(4):964–70.
[28] Jones JR, Hench LL. Regeneration of trabecular bone using porous ceramics. Curr Opin Solid State Mater Sci 2003;7: 301–7.